Scientific Research Publishing

Journal of Power and Energy Engineering, 2024, 12, 63-83
https://www.scirp.org/journal/jpee
ISSN Online: 2327-5901
ISSN Print: 2327-588X

Optimizing Power Flow in Northern Cameroon's Interconnected Grid: Challenges and Solutions

Jean Ndoumbe[1], Ivan Basile Kabeina[1], Michael Koumbou Piembe[2], Martin Ndjock[2]

[1]Laboratory of Computer Engineering, Data Science and Artificial Intelligence, National Higher Polytechnic School of Douala, University of Douala, Douala, Cameroon
[2]Laboratory of Electronics, Electrotechnics, Automation and Telecommunications, National Higher Polytechnic School of Douala, University of Douala, Douala, Cameroon
Email: jndoumbe02@gmail.com

How to cite this paper: Ndoumbe, J., Kabeina, I.B., Piembe, M.K. and Ndjock, M. (2024) Optimizing Power Flow in Northern Cameroon's Interconnected Grid: Challenges and Solutions. *Journal of Power and Energy Engineering*, **12**, 63-83.
https://doi.org/10.4236/jpee.2024.129005

Received: August 15, 2024
Accepted: September 16, 2024
Published: September 19, 2024

Abstract

This paper presents an analysis of the power flow within the Northern Interconnected Grid of Cameroon. The Newton-Raphson method has been performed, known for its accuracy, under MATLAB software, to model and solve complex power flow equations. This study simulates a series of outage scenarios to evaluate the responsiveness of the grid. The results obtained underline the crucial importance of reactive power management and highlight the urgent need to consolidate the grid infrastructure of North Cameroon. To increase grid resilience and stability, the paper recommends the strategic integration of renewables and the development of interconnections with other power grids. These measures are presented as viable solutions to meet current and future energy distribution challenges, ensuring a reliable and sustainable power supply for Cameroon.

Keywords

Power Flow, Northern Interconnected Grid, Newton-Raphson, MATLAB, Grid Stability

1. Introduction

Cameroon, like many developing countries, is facing major challenges in managing its electricity system. These challenges are exacerbated by growing energy demand, aging infrastructure, and financial constraints. The situation is particularly critical in the country's three main electricity grids: the Eastern Interconnected Grid (EIG), the Northern Interconnected Grid (NIG) and the Southern

Interconnected Grid (SIG). Each of these networks presents unique problems, influenced by geographical, economic and technical factors.

For example, the NIG suffers from a production deficit and the saturation of its transmission network. Indeed, population growth in northern Cameroon over the past two decades has led to a significant increase in electricity demand, exacerbating access issues, especially in rural areas [1]. Energy production is also affected by unfavourable hydrological conditions, as evidenced by the declining water level in the reservoirs of the Lagdo hydropower plant, leading to the shutdown of turbines due to lack of maintenance [2].

This situation has resulted in the transmission grid being utilized in ways not originally anticipated, leading to a series of unplanned occurrences. These include power outages, which have been attributed to the escalating demand on the system and alterations in its operational procedures [3]. The increasing load and operational changes have put unexpected stress on the power infrastructure, highlighting the need for adaptive strategies in managing and upgrading the grid to ensure reliability and efficiency [4].

Power flow analysis serves as a critical tool in addressing issues pertaining to power disruptions and ensuring the power grid's optimal functionality. Its primary objective is to ascertain the electrical status of the grid, a vital aspect for the effective management and operation of power systems [5]. This analysis is instrumental in identifying the voltages and currents across the network segments, confirming that the equipment functions within secure and stable parameters. By pinpointing areas of power losses and potential overloads, it enhances the utilization of generators and transmission lines. Moreover, it furnishes vital information necessary for the strategic planning of new facilities and the grid's augmentation, thereby guaranteeing an efficient electricity distribution. Furthermore, power flow analysis contributes to the reduction of operational costs by reducing losses and improving efficiency [6].

A standard power flow analysis yields key parameters such as the voltage magnitude and phase angle at each bus bar, along with the active and reactive power transfers between buses. Solving the power flow equations determines the network's steady-state voltage conditions for each bus bar. However, these equations are inherently nonlinear, making mathematical solutions challenging to derive.

Several researchers have tried the linearization approach of power flow equations. Bolognani and Zampieri [7] proposed a linear approximation of the power flow equations, valid for generic line impedances and network topology. However, real distribution networks can have more complex topologies and features than those modelled, making the direct application of theoretical results more difficult. Garces [8] proposed a linear load flow method for three-phase power distribution systems, which is accurate and applicable to both balanced and unbalanced systems, using a complex-plane linear approximation. Limitations of this method include reduced accuracy with high constant power loads and very low voltages, as well as the failure to consider PV nodes and other common controls in power distribution systems. Liu, *et al.* [9] proposed a data-driven approach

to linearize power flow models, using regression algorithms to improve the accuracy of calculations. Although this approach reduces complexity compared to nonlinear methods, it can still be computationally demanding for large power systems.

The Gauss-Seidel and Newton-Raphson techniques remain predominant for the analysis of power flows. The former is preferred for its simplicity and effectiveness in scenarios where a well-chosen initial assumption can lead to convergence. For example, Chamim, *et al.* [10] used the Gauss-Seidel approach to examine the energy flow in Bali's 150 kV radial power grid. However, when it comes to power flow studies, the Newton-Raphson method is often considered more robust and powerful than the Gauss-Seidel method [11] [12]. This is mainly due to the rapid convergence rate of the Newton-Raphson method, which is particularly advantageous when dealing with very nonlinear and complex equations.

This paper focuses on the analysis of power flow within the NIG, by applying the Newton-Raphson method via the MATLAB software. Various failure scenarios were replicated to examine the network's response to these incidents. The second section describes the northern interconnected network and how it is represented. The third section describes the methods used to model power flow. This same section also discusses the strategy adopted to solve power flow equations, using the Newton-Raphson method. The fourth section is devoted to the presentation of the results obtained, as well as to their analysis and discussion. Finally, the sixth section offers a general conclusion of the study.

2. Grid Overview and Modelling

2.1. Grid Overview

The NIG is instrumental in the distribution of energy generated in the country's northern region (**Figure 1**). It facilitates the transfer of power from the Lagdo

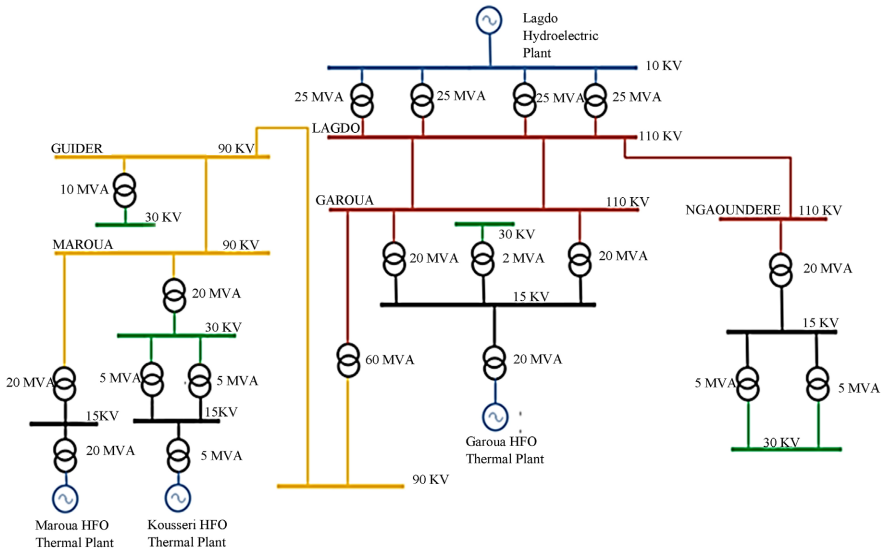

Figure 1. NIG single-line diagram.

hydroelectric plant, situated on the Benoue River approximately 66 kilometres from Garoua. The Lagdo facility boasts a considerable storage capacity of 6,300 million cubic meters and spans an area of 700 square kilometres. It consists of four 18 MW units, culminating in a combined capacity of 72 MW and an estimated annual output of 250 GWh. Beyond the Lagdo plant, the NIG also conveys power from the Djamboutou thermal station located near Garoua, which operates on Light Fuel Oil and has a capacity of 20 MW. Additional plants include a 10 MW station in Maroua and a 4.2 MW station in Kousseri, although their output is significantly less. The grid itself is comprised of 400 kilometres of 110 kV transmission lines and 200 kilometres of 90 kV lines, delivering electricity to the urban centres of Garoua, Maroua, Ngaoundéré, and Meiganga, thus playing a pivotal role in meeting the energy needs of these cities. Table 1 shows the installed grid connected generation capacities for the NIG.

Table 1. Installed grid generation capacity.

Plant name	Fuel Type	Installed capacity (MW)
Lagdo	hydro	72
Garoua	HFO	20
Maroua	HFO	10
Kousseri	HFO	4

2.2. Grid Modelling

Modelling large-scale power transmission systems often involves simplification to make calculations more manageable. By decreasing the dimensionality of the grid, the time required for simulations can be significantly reduced while maintaining acceptable accuracy. This simplification is typically achieved by consolidating multiple nodes into one and recalculating the capacities for equivalent transmission lines. This approach allows for performance optimization without sacrificing the quality of the results obtained.

The four generators, like the four transformers, share identical characteristics and their parallel configuration allows them to be considered as a single generator or transformer.

Two lines connect the source node of Lagdo to the node of Garoua. When two power lines run in parallel, their behaviour can effectively be represented by a single line with an equivalent impedance, which is calculated based on the individual impedances of the original lines.

This approach reduces the complexity of the network to make it easier to compute and understand the behaviour of the system. By replacing each component with its theoretical model, and focusing only on significant loads, such as those at the 110 kV and 90 kV nodes, a more abstract and manageable representation of the network is obtained. Figure 2 illustrates the simplified topology of the NIG, highlighting the key elements and connections between them, while omitting non-essential details for a clear overview.

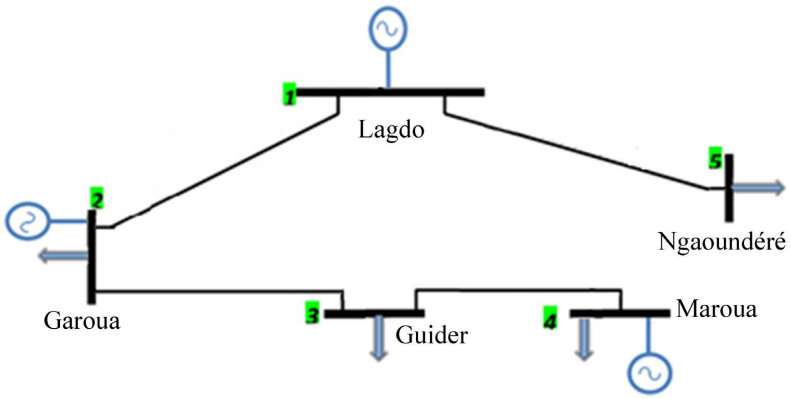

Figure 2. Simplified topology of NIG.

2.3. Line Parameters

Calculating the parameters and characteristics of power lines is particularly important for power system analysis.

The calculation of the DC line resistance at a temperature of 20˚C is:

$$R_C = \rho \frac{l}{s} \tag{1}$$

With:

l	Length of the line (m).
s	Conductor section (m^2).
ρ	Resistivity of metal (aluminium) (Ωm).

The resistivity is a function of the temperature θ and is written by:

$$\rho(\theta) = \rho(\theta_0)\left[1+(\theta-\theta_0)\right] \tag{2}$$

With $\alpha = 4\times10^{-3}\,^{\circ}\mathrm{C}^{-1}$copper and aluminium, θ_0 being the reference temperature (20˚C).

The resistance of a twisted DC conductor exceeds that calculated by the R_C formula. This difference is due to the increased length of the spiral wires, which is longer than the straight conductor. The increase in strength is approximately 1% for conductors composed of three wires and reaches about 2% for those with concentric strands. The AC resistance RA is determined as a function of R_C using the Kelvin ratio given by:

$$q = \pi d\sqrt{\frac{2f\times10^{-5}}{\rho}} \tag{3}$$

With:

d	Conductor diameter (mm).
f	Frequency of the network (Hz).
ρ	Resistivity of the metal (Ω·mm^2/km)

To calculate the reactance of a three-phase power line, it is essential to determine the inductance of the line. In the case of a symmetrical three-phase line, where the conductors are arranged at the vertices of an equilateral triangle, the inductance can

be calculated by considering the geometry of the conductors and the uniform distance between them. Considering that the conductors have identical radii, and that the distance between each pair of conductors is equal, then the linear reactance X can be estimated using standardized formulas that consider these parameters.

The inductance L (H/km) of a line is given by:

$$L = 2\times10^{-7} \ln\frac{D}{re^{-1/4}} \tag{4}$$

With:

D the inter-distance between each two conductors.

R conductor's radius.

The Inductive reactance $X(\Omega)$ is:

$$X = 2\pi fL \tag{5}$$

The capacity C (F/km) of the line can be calculated as:

$$C = \frac{1}{1.798\times10^{-7} \ln\left(\frac{D}{re^{-1/4}}\right)} \tag{6}$$

To model the average length power line, we use the line impedance $\overline{Z}$ and the line admittance $\overline{Y}$ such as:

$$\overline{Z} = (R + jX)l \tag{7}$$

$$\frac{\overline{Y}}{2} = j2\pi fC \tag{8}$$

For the short line model, $\overline{Y}$ is negligible.

Table 2 presents the parameters of the simplified network of the NIG. The per unit system is used in this modelling to express the quantities of the system as fractions of a defined base unit quantity. This approach simplifies calculations by ensuring that quantities remain constant when processed on different sides of a transformer, which is especially beneficial in scenarios involving many transformers. It also allows for the comparison of several types of equipment on a common scale, as impedances and other parameters are usually within a narrow range when expressed in unit values, regardless of the actual size of the equipment.

3. Power Flow Modelling

3.1. Buses Classification

An electrical system is defined by datasets about the nodes and lines in the network. Each i node is associated with four essential parameters: the voltage magnitude V_i, the voltage phase angle δ_i, the active power P_i and the reactive power Q_i injected. For each node, two of these variables are predetermined while the other two must be calculated. When analysing power flows, buses are divided into three distinct categories as shown in Table 3.

The slack bus is responsible for balancing the active and reactive power in the system by accounting for the difference between the total generated power and

the total system load, including losses. Essentially, it acts as a buffer, absorbing or supplying power to maintain equilibrium within the electrical network. This ensures stability and reliable operation of the power grid. The slack bus is commonly considered as the reference bus because both voltage V and angle δ are specified, the powers P and Q are to be determined. Usually identified by the number 1, its voltage magnitude and angle remain constant, while its active and reactive powers require calculation.

The regulated buses are the rest of generator buses. In this type of node, the real powers P_i and the voltage magnitude V are known and controllable. On the other hand, the reactive power Q_i and the phase angle of voltage δ remain to be determined.

The load buses are buses with fixed P and Q powers, the voltage magnitude V and the angle δ are unknown. Most of the buses in practical power systems are load buses [13]. PQ buses are characterized by unknown voltage magnitudes and angles, contrasting with PV buses where only the voltage angle remains undetermined.

The Slack bus, however, has predetermined voltage magnitudes and angles, eliminating the need to solve for any variables. Within a network comprising n buses and g generators, the total number of unknowns is calculated as $2(n-1)-(g-1)$ [13]. The resolution of these unknowns is facilitated through the application of real and reactive power balance equations. These critical equations are formulated based on the transmission network's representation via the admittance matrix, commonly referred to as Y-bus. This matrix is pivotal in analysing the flow of electrical power through the network and is instrumental in the stability and control of power systems. It serves as the foundation for various algorithms designed to ensure efficient operation and management of the electrical grid. The admittance matrix encapsulates the complex interplay between the network's buses and lines, providing a comprehensive framework for addressing the intricate challenges inherent in power system analysis [14]. The data used for this study were obtained from IED [15] and are presented in **Table 4**.

Table 2. Line parameters of NIG.

From bus	To bus	Length (km)	R (pu)	X (pu)
1	5	238	0.1641	0.7586
1	2	50	0.0742	0.1691
2	3	101	0.1670	0.4994
3	4	99	0.1637	0.4896

Table 3. Type of buses in the power flow problem [13].

Bus type	Voltage ($\lvert V_i \rvert \angle \delta_i$)		Real power			Reactive power		
	Magnitude	Angle	Generation	Load	Net (P_i)	Generation	Load	Net (Q_i)
Slack/Swing	Specified	Specified	Unknown	Specified	Unknown	Unknown	Specified	Unknown
Generator/	Specified	Unknown	Specified	Specified	Specified	Unknown	Specified	Unknown
Regulated/PV	Unknown	Unknown	Specified	Specified	Specified	Specified	Specified	Specified

Table 4. Bus data of NIG.

Bus	Type	V (pu)	Phase (pu)	P_gen (MW)	Q_gen (MVAR)	P_load (MW)	Q_load (MVAR)	Q_injected (MVAR)
1	Slack	1	0	-	-	0	0	0
2	PV	1	-	0.2	-	0.29	0.13	0
3	PQ	-	-	0	0	0.05	0.02	0
4	PV	1	-	0.142	-	0.42	0.07	0
5	PQ	-	-	0	0	0.13	0.03	0

3.2. Admittance Equation

The admittance matrix, or Y-bus, is a fundamental component in power system analysis. It is the complex admittance of the components in a power network, allowing for the analysis of power flow and voltage distribution. The symmetry along the diagonal is due to the mutual admittance between buses being equal in both directions, reflecting the physical reality of power systems where power can flow bidirectionally between nodes. The Y-bus is given by:

$$Y = \begin{bmatrix} Y_{11} & \cdots & Y_{1n} \\ \vdots & \ddots & \vdots \\ Y_{n1} & \cdots & Y_{nn} \end{bmatrix} \tag{9}$$

The elements of the diagonal are written as:

$$Y_{ii} = \sum_{\substack{j=0 \\ j \neq i}}^{n} y_{ij} \tag{10}$$

The elements outside the diagonal are written as:

$$Y_{ij} = Y_{ji} = -y_{ij} \tag{11}$$

3.3. Power Flow Equation

Equation (12) is the polar form of the power flow equations, formulated for an n-bus system as a function of the intake matrix of the Ybus, with reference to **Figure 3** [13].

$$I_i = V_i y_{i0} + (V_i - V_1) y_{i1} + (V_i - V_2) y_{i2} + \cdots + (V_i - V_j) y_{ij} \tag{12}$$

Grouping the elements as a function of the voltage, Equation (2) becomes as follows:

$$I_i = V_i (y_{i0} + y_{i1} + y_{i2} + \cdots + y_{ij}) - V_1 y_{i1} - V_2 y_{i2} - \cdots - V_j y_{ij} \tag{13}$$

Even better,

$$I_i = V_i \sum_{\substack{j=0 \\ j \neq i}} y_{ij} - \sum_{\substack{j=1 \\ j \neq i}} y_{ij} V_j \tag{14}$$

Either

$$I_i = V_i y_{ii} + \sum_{\substack{j=1 \\ j \neq i}} y_{ij} V_j \tag{15}$$

The power equation at a given bus is expressed in the following manner [16]:

$$S_i = P_i + jQ_i = V_i I_i^* \tag{16}$$

Or

$$S_i^* = P_i - jQ_i = V_i^* I_i \tag{17}$$

Thus, we can write, by inserting Equation (15) into Equation (17):

$$S_i^* = P_i - jQ_i = V_i^* \left(V_i Y_{ii} + \sum_{\substack{j=1 \\ j \neq i}} Y_{ij} V_j \right) \tag{18}$$

By introducing the polar forms, we obtain:

$$S_i^* = P_i - jQ_i = |V_i| \angle(-\delta_i) \left(|V_i||Y_{ii}| \angle(\delta_i) + \sum_{\substack{j=1 \\ j \neq i}} |Y_{ij}||V_j| \angle(\theta_{ij} + \delta_j) \right) \tag{19}$$

And finally:

$$S_i^* = P_i - jQ_i = \sum_{\substack{j=1 \\ j \neq i}} |Y_{ij}||V_i||V_j| \angle(\theta_{ij} - \delta_i + \delta_j) \tag{20}$$

The active and reactive powers are deduced respectively as follows:

$$P_i = \sum_{j=1}^{n} |V_i||V_j||Y_{ij}| \cos(\theta_{ij} - \delta_i + \delta_j) \tag{21}$$

$$Q_i = -\sum_{j=1}^{n} |V_i||V_j||Y_{ij}| \sin(\theta_{ij} - \delta_i + \delta_j) \tag{22}$$

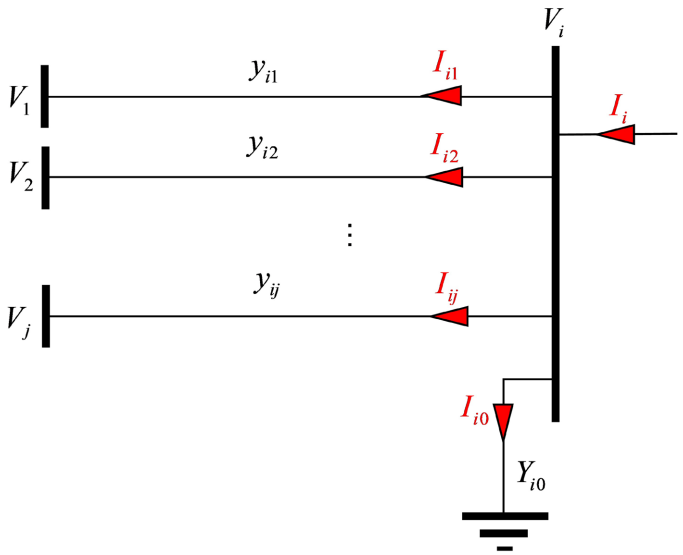

Figure 3. Typical power system bus bar model [13].

3.4. Newton-Raphson Technique

The Newton-Raphson (N-R) technique, also known as the method of successive approximation, is based on Taylor's expansion approximation [13]. Applying

Taylor's expansion to the Equations (21) and (22), we obtain:

$$P_i^{sch} = P_i^k + \sum_{j=2}^{n} \frac{\partial P_i^k}{\partial \delta_i} \partial \delta_i + \sum_{j=2}^{n} \frac{\partial P_i^k}{\partial |V_i|} \partial V_i \tag{23}$$

$$Q_i^{sch} = Q_i^k + \sum_{j=2}^{n} \frac{\partial Q_i^k}{\partial \delta_j} \partial \delta_j + \sum_{j=2}^{n} \frac{\partial Q_i^k}{\partial |V_j|} \partial |V_j| \tag{24}$$

In Equations (23) and (24), the inconnue variables are both voltage magnitude and angles $|V_i| \angle \delta_i$ at load buses, and the angles δ_i at regulated buses. P_i^{sch} and Q_i^{sch} are respectively the scheduled values of active power at the generator bus and the load and reactive power at load buses. We can write:

$$\Delta P_i^k = P_i^{sch} - P_i^k = \sum_{j=2}^{n} \frac{\partial P_i^k}{\partial \delta_j} \partial \delta_j + \sum_{j=2}^{n} \frac{\partial P_i^k}{\partial |V_j|} \partial V_j \tag{25}$$

$$\Delta Q_i^k = Q_i^{sch} - Q_i^k = \sum_{j=2}^{n} \frac{\partial Q_i^k}{\partial \delta_j} \partial \delta_j + \sum_{j=2}^{n} \frac{\partial Q_i^k}{\partial |V_j|} \partial |V_j| \tag{26}$$

The use of the matrix expression leads us to:

$$\begin{bmatrix} \Delta P_i^k \\ \Delta Q_i^k \end{bmatrix} = \begin{bmatrix} \dfrac{\partial P_i^k}{\partial \delta_j} & \dfrac{\partial P_i^k}{\partial |V_j|} \\ \dfrac{\partial Q_i^k}{\partial \delta_j} & \dfrac{\partial Q_i^k}{\partial |V_j|} \end{bmatrix} \begin{bmatrix} \Delta \delta_j^k \\ \Delta V_j^k \end{bmatrix} = \begin{bmatrix} J_{P\delta} & J_{P|V|} \\ J_{Q\delta} & J_{Q|V|} \end{bmatrix} \begin{bmatrix} \Delta \delta_j^k \\ \Delta V_j^k \end{bmatrix}, \ i, j = 2, \cdots, n \tag{27}$$

We deduce that:

$$\begin{bmatrix} \Delta \delta_j^k \\ \Delta V_j^k \end{bmatrix} = \begin{bmatrix} J_{P\delta} & J_{P|V|} \\ J_{Q\delta} & J_{Q|V|} \end{bmatrix}^{-1} \begin{bmatrix} \Delta P_i^k \\ \Delta Q_i^k \end{bmatrix}, \ i, j = 2, \cdots, n \tag{28}$$

So, new values are calculated by:

$$\begin{bmatrix} \delta_j^k \\ V_j^k \end{bmatrix} = \begin{bmatrix} \delta_j^{k-1} \\ V_j^{k-1} \end{bmatrix} + \begin{bmatrix} \Delta \delta_j^k \\ \Delta V_j^k \end{bmatrix} \tag{29}$$

The iterative process stops when:

$$\begin{bmatrix} \Delta \delta_j^k \\ \Delta V_j^k \end{bmatrix} \leq precision \tag{30}$$

Figure 4 shows the Newton-Raphson algorithm, implemented in the MATLAB/Simulink software.

3.5. IEEE-14 Bus Test System

The IEEE-14 Bus system is a commonly used test case for researchers and engineers in the field of electrical power systems. It serves as a benchmark for testing new algorithms and methods for system analysis and optimization. The system consists of 14 buses, 20 transmission lines, and 11 loads, representing a small-scale model of a real-world power system (Figure 5). Table 5 and Table 6 provide the details of buses data and branches data for the IEEE-14 Bus system [17].

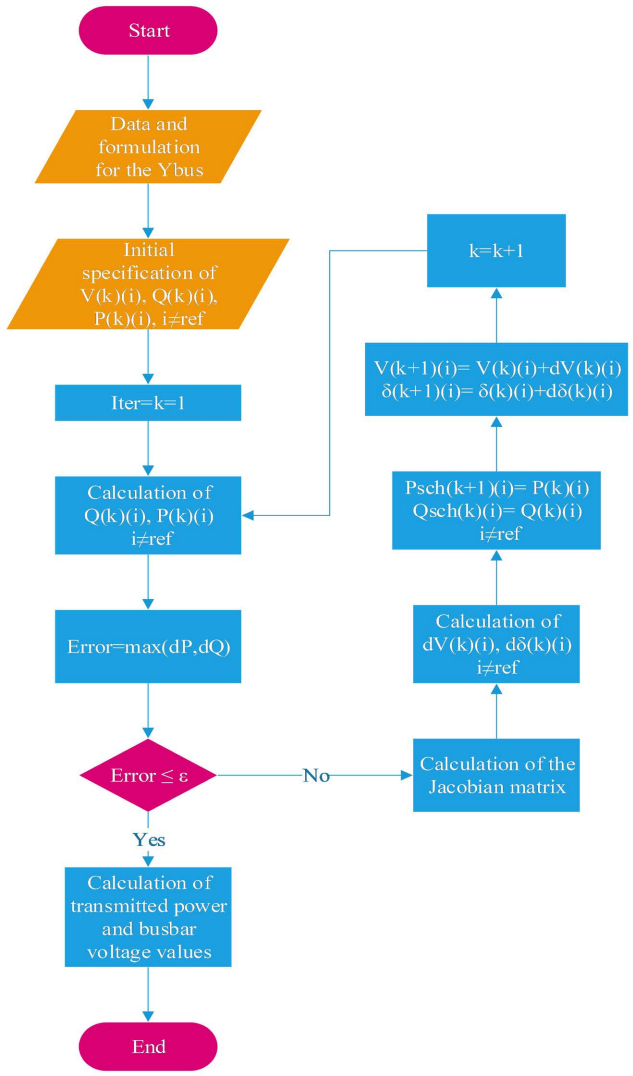

Figure 4. Newton-Raphson algorithm.

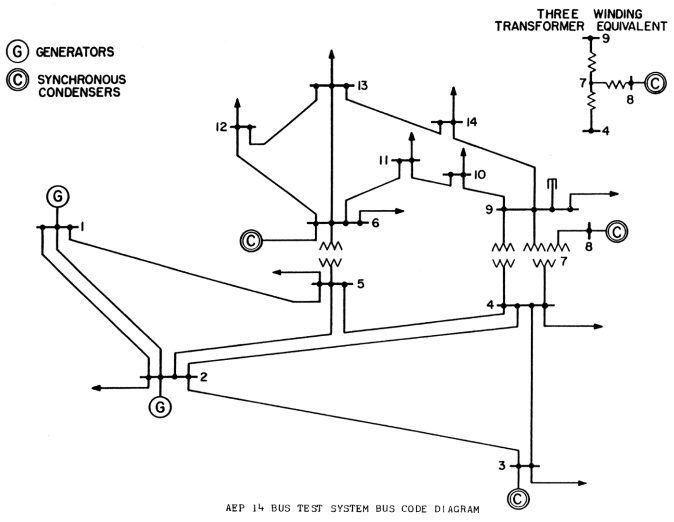

Figure 5. IEEE-14 bus system [17].

Table 5. Bus data of IEEE-14 bus system [17].

Bus	Type	V (pu)	Phase (pu)	P_gen (MW)	Q_gen (MVAR)	P_load (MW)	Q_load (MVAR)	Q_injected (MVAR)
1	Slack	1.0600	0	0	0	0	0	0
2	PV	1.0450	0	40	0	21.7000	12.7000	0
3	PV	1.0100	0	0	0	94.2000	19	0
4	PQ	0	0	0	0	47.8000	−3.9000	0
5	PQ	0	0	0	0	7.6000	1.6000	0
6	PV	1.0700	0	0	0	11.2000	7.5000	0
7	PQ	0	0	0	0	0	0	0
8	PV	1.0900	0	0	0	0	0	0
9	PQ	0	0	0	0	29.5000	16.6000	19
10	PQ	0	0	0	0	9	5.8000	0
11	PQ	0	0	0	0	3.5000	1.8000	0
12	PQ	0	0	0	0	6.1000	1.6000	0
13	PQ	0	0	0	0	13.5000	5.8000	0
14	PQ	0	0	0	0	14.9000	5	0

Table 6. Branch data of IEEE-14 bus system [17].

From bus	To bus	R (pu)	X (pu)
1	2	0.0194	0.0592
1	5	0.0540	0.2230
2	3	0.0470	0.1980
2	4	0.0581	0.1763
2	5	0.0570	0.1739
3	4	0.0670	0.1710
4	5	0.0134	0.0421
4	7	0	0.2091
4	9	0	0.5562
5	6	0	0.2520
6	11	0.0950	0.1989
6	12	0.1229	0.2558
6	13	0.0662	0.1303
7	8	0	0.1762
7	9	0	0.1100
9	10	0.0318	0.0845
9	14	0.1271	0.2704
10	11	0.0820	0.1921
12	13	0.2209	0.1999
13	14	0.1709	0.3480

4. Results and Discussions

4.1. Algorithm Test on IEEE-14 Bus System

The IEEE-14 bus system provides a robust framework for testing and validating new methodologies and software implementations. Table 7 presents the results of the application of the Newton-Raphson algorithm on IEEE-14 buses. The total real power and reactive power loads are 272.39 MW and 82.44 Mvar respectively. The conformity of the results obtained with those published by other researchers reinforces the validity of the Newton-Raphson algorithm developed under Matlab [17]-[19].

Table 7. Results of power flow of IEEE-14 bus system.

No_Bus	V (pu)	Phase (pu)	P_gen (MW)	Q_gen (MVAR)	P_load (MW)	Q_load (MVAR)
1	1.0600	0	232.3933	−16.5493	0	0
2	1.0450	−4.9826	40.0000	43.5571	21.7000	12.7000
3	1.0100	−12.7251	0	25.0753	94.2000	19
4	1.0177	−10.3129	0	0	47.8000	−3.9000
5	1.0195	−8.7739	0	0	7.6000	1.6000
6	1.0700	−14.2209	0	12.7309	11.2000	7.5000
7	1.0615	−13.3596	0	0	0	0
8	1.0900	−13.3596	0	17.6235	0	0
9	1.0559	−14.9385	0	0	29.5000	16.6000
10	1.0510	−15.0973	0	0	9	5.8000
11	1.0569	−14.7906	0	0	3.5000	1.8000
12	1.0552	−15.0756	0	0	6.1000	1.6000
13	1.0504	−15.1563	0	0	13.5000	5.8000
14	1.0355	−16.0336	0	0	14.9000	5
	Total		272.3933	82.4375	259.0000	73.5000

4.2. Scenario 1: All Plants are Operating

Table 8 presents the results of the NIG power flow. All voltage drops do not exceed 10% of their nominal value. So, in this scenario, all busbars meet the standard. To ensure the balance of the system, the slack bus, which is here the Lagdo hydroelectric power plant, must produce a power of 61.02 MW or 84.75% of the installed capacity. However, it also must absorb a reactive power of 22.78 MVar, which represents a loss factor of 34.97%. This underscores the importance of reactive power management to maintain grid efficiency and stability. These results show that the Lagdo plant is essential for the balance of the NIG. However, the loss factor of 34.97% indicates that there is significant improvement in terms of

reactive power management, including the integration of reactive power compensation devices. The results of the power flow along the lines of the NIG are presented in Table 9. The Lagdo-Ngaoundéré and Garoua-Guider lines are the most overcrowded, but the power transmitted remains acceptable.

Table 8. Results of power flow of NIG.

No_Bus	V (pu)	Phase (pu)	P_gen (MW)	Q_gen (MVAR)	P_load (MW)	Q_load (MVAR)
1	1	0	61.0175	−22.7774	0	0
2	1	−5.4040	20.0000	29.3023	29	13
3	0.9796	−16.6583	0	0	5	2
4	1	−26.2229	14.2000	22.1575	42	7
5	0.9803	−5.8643	0	0	13	3
	Total		95.2175	28.6824	89	25

Table 9. Power flow on NIG lines.

From bus	To bus j	Pij (MW)	Qij (MVAR)	P_loss (MW)	Q_loss (MVAR)	S_loss (MVA)
1	5	13.2899	−3.6989	0.2899	−6.6989	6.7051
1	2	47.7276	−19.0785	1.9326	2.7937	3.3970
2	3	36.7949	−5.5699	2.294	4.6653	5.1987
3	4	29.5009	−12.2352	1.7009	2.9223	3.3812
		Total		6.2175	3.6824	7.2262

4.3. Scenario 2: The Garoua Power Plant Is Out of Service

The results of the NIG power flow when the Garoua power plant is out of service are shown in Table 10. There is a drop in voltage in all the buses in the network. The drop in voltage is more significant at the Garoua bus. This generalized voltage drop could indicate a significant dependence of the grid on the Garoua power plant. In addition, it underscores the strategic importance of the Garoua power plant to maintain the stability of the grid voltage. However, the voltage remains acceptable to all buses despite the decrease, which shows that the network has a certain resilience, even if it should be strengthened.

However, this scenario, in which power demand exceeds the production capacity of the Lagdo plant, has several implications and requires specific measures to optimize production while ensuring safety (Table 11). Indeed, the Lagdo plant would be overloaded, which can lead to premature wear and tear of the equipment, increasing the risk of breakdowns and failures. In addition, overloading can cause voltage fluctuations, affecting the quality of the power supply to consumers. To avoid overloading, it may be necessary to set up load shedding, which will certainly lead to power cuts for some users.

Table 10. Power flow behaviour of NIG when Garoua Power Plant is out of service.

No_Bus	V (pu)	Phase (pu)	P_gen (MW)	Q_gen (MVAR)	P_load (MW)	Q_load (MVAR)
1	1	0	84.0371	6.3937	0	0
2	0.9359	−6.8421	0	0	29	13
3	0.9423	−20.2635	0	0	5	2
4	1	−31.0465	14.2000	30.4009	42	7
5	0.9803	−5.8643	0	0	13	3
	Total		98.2371	36.7946	89	25

Table 11. Power flow on NIG lines when Garoua Power Plant is out of service.

From bus	To bus j	Pij (MW)	Qij (MVAR)	P_loss (MW)	Q_loss (MVAR)	S_loss (MVA)
1	5	13.2899	−3.6989	0.2899	−6.6989	6.7051
1	2	70.7472	10.0926	3.7918	7.1401	8.0844
2	3	37.9554	−10.0475	2.9035	6.7072	7.3087
3	4	30.0519	−18.7547	2.2519	4.6462	5.1632
	Total			9.2371	11.7946	14.9812

4.4. Scenario 3: The Maroua Power Plant Is Out of Service

The results of the power flow (Table 12) of the NIG when the Maroua power plant is out of service also show a voltage drop in all the buses in the network, more marked at the Garoua bus. This indicates a significant dependence of the grid on this thermal power plant and highlights its strategic importance for voltage stability.

Table 12. Power flow behaviour of NIG when Maroua Power Plant is out of service.

No_Bus	V (pu)	Phase (pu)	P_gen (MW)	Q_gen (MVAR)	P_load (MW)	Q_load (MVAR)
1	1	0	76.0840	−27.5014	0	0
2	1	−7.0731	20.0000	38.9393	29	13
3	0.9639	−22.5126	0	0	5	2
4	1	−36.1358	4.2000	31.4820	42	7
5	0.9803	−5.8643	0	0	13	3
	Total		100.2840	42.9199	89	25

Table 13 presents the power flow on NIG lines when Maroua Power Plant is out of service. The results show that there is an overload of the Lagdo hydroelectric power plant, thus increasing the risk of outages and voltage fluctuations, which would affect the quality of the power supply. To avoid overloading, it may also be necessary to set up load shedding.

Table 13. Power flow on NIG lines when Maroua Power Plant is out of service.

From bus	To bus j	Pij (MW)	Qij (MVAR)	P_loss (MW)	Q_loss (MVAR)	S_loss (MVA)
1	5	13.2899	0.2899	0,2899	−6.6989	6.7051
1	2	62.7941	3.3091	3,3091	5.9373	6.7971
2	3	50.485	4.2684	4,2684	10.6037	11.4305
3	4	41.2166	3.4166	3,4166	8.0778	8.7706
Total				11.284	17.9199	21.1766

4.5. Scenario 4: The Kousseri Power Plant Is Out of Service

Table 14 illustrates the energy flow results for the NIG when the Kousseri power plant is offline. It reveals a minor voltage drop across all network buses. The failure of this low-power plant leads to an increase in reactive power generated by other plants. This indicates that these plants must compensate not only for the loss of active power but also for the increased demand for reactive power, which can impact their performance and efficiency. These findings highlight the electrical network's resilience. Despite the shutdown of a power plant, the network manages to offset the power loss, albeit with a slight voltage drop and an increase in reactive power.

Table 14. Power flow behaviour of NIG when Kousseri Power Plant is out of service.

No_Bus	V (pu)	Phase (pu)	P_gen (MW)	Q_gen (MVAR)	P_load (MW)	Q_load (MVAR)
1	1	0	67.0801	−24.7363	0	0
2	1	−6.0775	20.0000	32.9034	29	13
3	0.9739	−19.0197	0	0	5	2
4	1	−30.2233	10.0000	25.7458	42	7
5	0.9803	−5.8643	2.1316e−14	1.5987e−14	13	3
	Total		97.0801	33.9129	89	25

This outage highlights the vulnerability of the NIG in the face of the loss of large sources of production as illustrated in Table 15. Despite the resilience of the grid, apparent power losses are increasing, which can lead to voltage imbalances and fluctuations. Although the grid is showing some adaptability, the increase in apparent power losses is a cause for concern. This can cause instabilities and voltage variations that could have repercussions on the distribution of electricity. It is therefore crucial to strengthen the robustness of the network to minimize the risk of failure and ensure a stable and reliable power supply for all users.

4.6. Discussions

The power flow analysis of Northern Cameroon's Interconnected Grid (NIG) provides crucial insights into the performance, stability, and efficiency of the

region's electrical network. The NIG relies on a combination of hydroelectric power and thermal plants. However, there can be a mismatch between generation capacity and demand, especially during peak periods or in dry seasons when hydroelectric production is low.

Table 15. Power flow on NIG lines when Kousseri Power Plant is out of service.

From bus	To bus j	Pij (MW)	Qij (MVAR)	P_loss (MW)	Q_loss (MVAR)	S_loss (MVA)
1	5	13.2899	−3.6989	0.2899	−6.6989	6.7051
1	2	53.7902	−21.0374	2.4439	3.9613	4.6545
2	3	42.3463	−5.0953	3.0211	6.852	7.4884
3	4	34.3253	−13.9473	2.3253	4.7986	5.3323
Total				8.0801	8.9129	12.0303

The results show that the NIG heavily relies on the Maroua and Garoua thermal power plants to maintain voltage stability. The shutdown of these plants leads to a generalized voltage drop, especially at the Garoua bus, highlighting their strategic importance. The overload of the Lagdo power plant under these conditions is concerning, as it can cause breakdowns, voltage fluctuations, and the need for load shedding. To optimize production and ensure safety, it is crucial to strengthen infrastructure, manage demand efficiently, and integrate additional energy sources [20]. Although the grid shows some resilience, measures are necessary to minimize the risk of failure and ensure a stable and reliable power supply for all users.

Improving the stability of the electricity grid is a major challenge to guarantee a reliable and continuous energy supply. The diversification of energy sources is a fundamental strategy in this regard. By integrating renewable energies such as solar, wind and hydropower, dependence on a single plant is reduced, while contributing to the energy transition to a more sustainable model [21] [22]. A study examining the integration of renewable energy in the electricity sector highlighted that solar PV emerges as the dominant technology in the energy mix by 2050 representing 86% of total annual generation, complemented by hydropower (8%) and sustainable bioenergy (5%) [23]. These renewables can contribute to the reduction of carbon emissions and fight climate change and create significant employment opportunities, with the potential to create more than 100,000 jobs by 2030 and more than 3 million jobs by 2050 in African countries [24].

Smart Grids represent a revolution in energy management. They enable real-time monitoring and optimization of power distribution, using advanced energy management technologies. Although implementation in Cameroon is still subject to several barriers, several researchers have proposed deployment methods [25]-[27]. By implementing these smart grids and advanced metering infrastructure, northern Cameroon will be able to optimize energy consumption, reduce waste and promote sustainable consumption patterns [28].

Finally, interconnections with other power grids provide an additional level of security: NIG is being strengthened and expanded to improve access to electricity and optimize energy exchanges with other networks. First, the interconnection project between the NIG and the SIG aims to create synergy between the two main electricity grids in Cameroon. This will strengthen the stability of the network and optimize the use of resources. Also, an interconnection project between Cameroon and Chad (PIRECT) was launched in November 2023, will allow the construction of 524 km of line between Ntui and Wouro Soua in Ngaoundéré, and 566 km of line from Wouro Soua in Chad via Garoua, Maroua, and Kousseri [29] [30].

However, the transition to a more sustainable energy grid is not without its challenges. The integration of renewable energy sources must be carefully managed to avoid potential negative environmental impacts, such as land-use changes and habitat disturbance [31]. In addition, there are economic considerations, including upfront capital costs and the need for ongoing maintenance and technical support [32].

5. Conclusion

The optimization of power flow in Northern Cameroon's Interconnected Grid is a critical task that addresses both current and future energy demands. The analysis reveals the complexities involved in balancing the grid, particularly in the face of aging infrastructure and the increasing need for stable electricity supply. The study highlights the effectiveness of computational techniques, such as the Newton-Raphson method, in managing these complexities by providing accurate and efficient solutions to power flow problems. The use of MATLAB for implementing the Newton-Raphson method has proven to be a powerful tool, offering flexibility and precision in modeling and simulation. The scenarios studied highlight the crucial importance of the Lagdo, Garoua, Maroua, and Kousseri power plants for grid stability. Diversifying energy sources, integrating renewable energies, and adopting smart grids are essential strategies to improve the resilience and efficiency of the grid. Interconnection projects with other grids, notably with the Southern Interconnected Grid and Chad, offer promising prospects for enhancing stability and optimizing the use of energy resources. The power flow analysis of Northern Cameroon's Interconnected Grid underscores the need for substantial investment in both infrastructure and technology. Addressing the identified challenges will be crucial for ensuring the reliability, efficiency, and sustainability of the power supply in the region. Additionally, aligning these technical improvements with broader socio-economic goals will be essential for the overall development of Northern Cameroon.

Acknowledgment

Deepest gratitude to Mr. Etienne Gbaweng Belporoh from the Government Technical High School of Ngaoundere for providing the field data that was instrumental

in the development of this work.

Conflicts of Interest

The authors declare no conflicts of interest regarding the publication of this paper.

References

[1] Njoh, A.J., Etta, S., Ngyah-Etchutambe, I.B., Enomah, L.E.D., Tabrey, H.T. and Essia, U. (2019) Opportunities and Challenges to Rural Renewable Energy Projects in Africa: Lessons from the Esaghem Village, Cameroon Solar Electrification Project. *Renewable Energy*, **131**, 1013-1021. https://doi.org/10.1016/j.renene.2018.07.092

[2] Kitmo,, Djidimbélé, R., Kidmo, D.K., Tchaya, G.B. and Djongyang, N. (2021) Optimization of the Power Flow of Photovoltaic Generators in Electrical Networks by MPPT Algorithm and Parallel Active Filters. *Energy Reports*, **7**, 491-505. https://doi.org/10.1016/j.egyr.2021.07.103

[3] Iweh, C.D., Gyamfi, S., Effah-Donyina, E. and Tanyi, E. (2024) Analysis of Contingency Scenarios Towards a Suitable Transmission Pathway in the Southern Interconnected Grid (SIG) of Cameroon. *e-Prime—Advances in Electrical Engineering, Electronics and Energy*, **7**, Article ID: 100486. https://doi.org/10.1016/j.prime.2024.100486

[4] Panteli, M., Trakas, D.N., Mancarella, P. and Hatziargyriou, N.D. (2017) Power Systems Resilience Assessment: Hardening and Smart Operational Enhancement Strategies. *Proceedings of the IEEE*, **105**, 1202-1213. https://doi.org/10.1109/jproc.2017.2691357

[5] Mouassa, S., Alateeq, A., Alassaf, A., Bayindir, R., Alsaleh, I. and Jurado, F. (2024) Optimal Power Flow Analysis with Renewable Energy Resource Uncertainty Using Dwarf Mongoose Optimizer: Case of ADRAR Isolated Electrical Network. *IEEE Access*, **12**, 10202-10218. https://doi.org/10.1109/access.2024.3351721

[6] Barnawi, A.B. (2024) Development and Analysis of AC Optimal Power Flow Optimization Algorithms for Minimization of Cost and Emissions with Stochastic Renewables. *Energy Reports*, **11**, 2059-2076. https://doi.org/10.1016/j.egyr.2024.01.052

[7] Bolognani, S. and Zampieri, S. (2016) On the Existence and Linear Approximation of the Power Flow Solution in Power Distribution Networks. *IEEE Transactions on Power Systems*, **31**, 163-172. https://doi.org/10.1109/tpwrs.2015.2395452

[8] Garces, A. (2016) A Linear Three-Phase Load Flow for Power Distribution Systems. *IEEE Transactions on Power Systems*, **31**, 827-828. https://doi.org/10.1109/tpwrs.2015.2394296

[9] Liu, Y., Zhang, N., Wang, Y., Yang, J. and Kang, C. (2019) Data-driven Power Flow Linearization: A Regression Approach. *IEEE Transactions on Smart Grid*, **10**, 2569-2580. https://doi.org/10.1109/tsg.2018.2805169

[10] Nazilah Chamim, A.N., Putra, K.T. and Al Farisi, M.F. (2023) Power Flow Analysis of Electrical Network Systems Using Gauss-Seidel Method and Python. *Emerging Information Science and Technology*, **4**, 28-36. https://doi.org/10.18196/eist.v4i1.18698

[11] Mohsin, M.Y., Khan, M.A.M., Yousif, M., Chaudhary, S.T., Farid, G. and Tahir, W. (2022) Comparison of Newton Raphson and Gauss Seidal Methods for Load Flow Analysis. *International Journal of Electrical Engineering & Emerging Technology*, **5**, 1-7.

[12] Abaali, H., Talbi, E. and Skouri, R. (2018) Comparison of Newton Raphson and Gauss Seidel Methods for Power Flow Analysis. *International Journal of Energy and Power*

Engineering, **12**, 627-633.

[13] Albadi, M. (2020) Power Flow Analysis. In: Volkov, K., Ed., *Computational Models in Engineering*, IntechOpen. https://doi.org/10.5772/intechopen.83374

[14] D'orto, M., Sjoblom, S., Chien, L.S., Axner, L. and Gong, J. (2021) Comparing Different Approaches for Solving Large Scale Power-Flow Problems with the Newton-Raphson Method. *IEEE Access*, **9**, 56604-56615. https://doi.org/10.1109/access.2021.3072338

[15] IED (2016) Plan Directeur d'Electrification Rurale du Cameroun (PDER)—Rapport final. Ministère de l'Eau et de l'Energie.

[16] Afolabi, O.A., Ali, W.H., Cofie, P., Fuller, J., Obiomon, P. and Kolawole, E.S. (2015) Analysis of the Load Flow Problem in Power System Planning Studies. *Energy and Power Engineering*, **7**, 509-523. https://doi.org/10.4236/epe.2015.710048

[17] ICSEG. IEEE 14-Bus System. https://icseg.iti.illinois.edu/ieee-14-bus-system/

[18] Hassan, H.A., Osman, Z.H. and Lasheen, A.E. (2014) Sizing of STATCOM to Enhance Voltage Stability of Power Systems for Normal and Contingency Cases. *Smart Grid and Renewable Energy*, **5**, 8-18. https://doi.org/10.4236/sgre.2014.51002

[19] Muzzammel, R., Khail, I., Tariq, M.H., Asghar, A.M. and Hassan, A. (2019) Design and Power Flow Analysis of Electrical System Using Electrical Transient and Program Software. *Energy and Power Engineering*, **11**, 186-199. https://doi.org/10.4236/epe.2019.114011

[20] Iweh, C.D., Gyamfi, S., Tanyi, E. and Effah-Donyina, E. (2021) Distributed Generation and Renewable Energy Integration into the Grid: Prerequisites, Push Factors, Practical Options, Issues and Merits. *Energies*, **14**, Article 5375. https://doi.org/10.3390/en14175375

[21] Kidmo, D.K., Deli, K. and Bogno, B. (2021) Status of Renewable Energy in Cameroon. *Renewable Energy and Environmental Sustainability*, **6**, Article No. 2. https://doi.org/10.1051/rees/2021001

[22] Amigue, F.F., Essiane, S.N., Ngoffe, S.P., Ondoa, G.A., Mengounou, G.M. and Nna Nna, P.T. (2021) Optimal Integration of Photovoltaic Power into the Electricity Network Using Slime Mould Algorithms: Application to the Interconnected Grid in North Cameroon. *Energy Reports*, **7**, 6292-6307. https://doi.org/10.1016/j.egyr.2021.09.077

[23] Manjong, N.B., Oyewo, A.S. and Breyer, C. (2021) Setting the Pace for a Sustainable Energy Transition in Central Africa: The Case of Cameroon. *IEEE Access*, **9**, 145435-145458. https://doi.org/10.1109/access.2021.3121000

[24] Bouchene, L., Cassim, Z., Engel, H., Jayaram, K. and Kendall, A. (2021) Green Africa: A Growth and Resilience Agenda for the Continent. How the Global Climate Agenda Creates Opportunities for Africa to Build Resilience, Catalyze Sustainable Growth, and Contribute to the Net-Zero Transition. https://www.mckinsey.com/capabilities/sustainability/our-insights/green-africa-a-growth-and-resilience-agenda-for-the-continent

[25] Camille, M., Alexandre, B. and Nneme Léandre, N. (2020) Roadmap for the Transformation of the South Cameroon Interconnected Network (RIS) into Smart-Grid. *American Journal of Energy Engineering*, **8**, 1-8. https://doi.org/10.11648/j.ajee.20200801.11

[26] Dandoussou, A., Kenfack, P. and Lekunze Toh, G. (2021) Distributed Generation and Optimization of Smart Grid Systems: Case Study of Kumba in Cameroon. *Trends Journal of Sciences Research*, **1**, 34-43. https://doi.org/10.31586/wjeee.2021.126

[27] Souhe, F.G.Y., Mbey, C.F., Boum, A.T. and Ele, P. (2021) Forecasting of Electrical

Energy Consumption of Households in a Smart Grid. *International Journal of Energy Economics and Policy*, **11**, 221-233. https://doi.org/10.32479/ijeep.11761

[28] Nyika, J. and Dinka, M.O. (2024) The Push for Renewable Energy Adoption in Africa. In: Asif, M., Sahin, G. and Khalid, M., Eds., *Handbook of Energy and Environment in the 21st Century*, CRC Press, 187-203. https://doi.org/10.1201/9781032715438-10

[29] Morella, E. (2021) Disclosable Version of the ISR-Cameroon-Chad Power Interconnection Project-P168185-Sequence No: 03. The World Bank.

[30] Kidmo, D.K., Bogno, B., Ngohe Ekam, P., Nisso, N. and Aillerie, M. (2022) Hydropower Generation Potential and Prospective Scenarios for Sustainable Electricity Supply for the Period 2022–2042: A Case Study of the NIN Zone of Cameroon. *Energy Reports*, **8**, 123-136. https://doi.org/10.1016/j.egyr.2022.06.090

[31] Azarpour, A., Suhaimi, S., Zahedi, G. and Bahadori, A. (2012) A Review on the Drawbacks of Renewable Energy as a Promising Energy Source of the Future. *Arabian Journal for Science and Engineering*, **38**, 317-328. https://doi.org/10.1007/s13369-012-0436-6

[32] Usman, F.O., Ani, E.C., Ebirim, W., Montero, D.J.P., Olu-lawal, K.A. and Ninduwezuor-Ehiobu, N. (2024) Integrating Renewable Energy Solutions in the Manufacturing Industry: Challenges and Opportunities: A Review. *Engineering Science & Technology Journal*, **5**, 674-703. https://doi.org/10.51594/estj.v5i3.865